

THE EFFECT OF FLOOR MEMBER SIZE ON THE
BEHAVIOR OF
REINFORCED CONCRETE BEAM-COLUMN JOINTS

by

Roberto T. Leon (I)
Presenting Author : Roberto T. Leon

SUMMARY

The results of an experimental program aimed at clarifying the effect of floor member size on the behavior of reinforced concrete beam-column joints in ductile moment-resisting frames (DMRF) are presented. The tests showed that the framing beam geometry and the presence of a floor slab can have a significant effect on the strength and hysteretic behavior of beam-column joints. The tests ascertained that the shear strength of joints may be high, and that in general flexural and bond considerations governed the behavior of the joints in the post-elastic range.

INTRODUCTION

Experimental and analytical work over the past 20 years has resulted in design recommendations and codes that ensure adequate strength and ductility for beams and columns in DMRF. For these frames to perform satisfactorily under severe earthquake loads, the beam-column joints must be able to transfer very large forces without appreciable deterioration of stiffness or strength. Because the "weak girder-strong column" design philosophy used for DMRFs requires yielding of the beams near or at the column face, very large shear and bond stresses may be introduced into the joint. If the deformations imposed are large, shear cracking of the joint and bond deterioration and slippage of the longitudinal reinforcement through the joint may be unavoidable unless proper precautions were taken in the design stage.

Although many experimental programs have been carried out on beam-column joints during the past 15 years (Ref. 1,2,3), many areas of joint design are still not clearly understood (Ref. 4). Among these areas are the effects of (1) 3D loading, (2) floor slabs, and (3) different size framing beams on overall joint behavior. This paper presents a short summary of a test series aimed at ascertaining the influence of floor members on the biaxial strength and hysteretic behavior of interior beam-column joints.

(I) Assistant Professor, U. of Minnesota, Minneapolis 55455

DESCRIPTION OF TEST SERIES

Since the tests were intended to demonstrate joint distress, the specimens were designed so that joint strength and stiffness would be critical in influencing subassemblage behavior. High joint shear, small anchorage lengths for the beam longitudinal bars, and minimum transverse joint shear reinforcement were intentionally used so that these problems could be observed. The specimens used were not intended to represent members in actual structures, and should not be considered to be typical of DMRFs as built today.

The typical specimen geometry and details are shown in Fig. 1, and the test series is summarized in Table 1. The specimens had heavily reinforced 15 by 15 in. columns, and beams with a constant depth of 18 in. and widths varying from 8.75 in. to 18 in. The floor slabs, when present, were 3.75 in. thick, and extended about 5 ft. around the joint. The joint core was confined by only 2 # 4 ties spaced at 5 in. , giving a joint volumetric reinforcement ratio of 1.33% .

Nominal material properties were 4.5 ksi for the concrete, and 60 ksi for the reinforcing steel. Beams in all specimens were designed to have similar flexural capacities, and the column to have a flexural overstrength of about 20% with respect to the beams. The actual moment ratios are shown in Table 1. The beams had the same reinforcement in both directions and the bars were displaced as necessary to pass through the joint region

Specimens BCJ5, BCJ11, and BCJ12, used to study the influence of beam size, were tested with an axial load of about 300 kips; this corresponded to the uniaxial balance axial load for the section. Specimens BCJ8 and BCJ9, used to study the effect of floor slabs, were tested without a column axial load.

The idealized deflected shape for an interior beam-column joint is shown in Fig. 2(a), while the testing scheme is shown in Fig. 2(b). Specimens were tested in an upright position, braced against a floor-wall reaction system, see Fig. 3, and loaded biaxially. Four vertical rods and centerhole rams applied the column axial load. Four rams with spherical end attachments, reacting against the test floor, loaded the beam ends up or down. The upper column was effectively pinned and braced to the reaction wall to resist the upper column shear. The bottom of the column was semi-rigidly connected to the reaction floor; a point of inflection formed a short distance above this connection to match approximately the idealized conditions shown in Fig. 2.

The specimens were subjected to a severe biaxial cyclic load history, shown in Fig.4. All the beam ends were originally deflected 0.1 in. downwards to simulate the effects of gravity loading. Cycling of the beams took place about this deflected position, and consisted of one short elastic cycle followed by three cycles at each of three progressively larger deflection levels. The first of these

deflection levels corresponded to the deformation at which first yielding was observed in the top longitudinal reinforcement. This was experimentally determined to be about 1.3 in from the gravity load position. This first deformation level corresponds to a uniaxial drift of about 2% and a ductility of about 3.0. The reader is urged to recall the severity of the loading when judging the specimen performance. The loads were applied biaxially simultaneously, with the North and West beams deflecting initially downwards and the South and East beams upwards.

The specimens were extensively instrumented to monitor deformations, loads, and reinforcement steel strains. Apparatuses were also devised to measure joint shear strain and longitudinal bar slip. All measurements were taken with a computer-controlled VIDAR data acquisition system.

EXPERIMENTAL RESULTS

The experimental results will be discussed utilizing the resultant beam moment-interstory displacement (MR vs. ID) relationships determined in the tests. The resultant beam moment is the vectorial sum of the beam moments at the columns face in the two orthogonal directions. The interstory drifts were calculated from the beam end displacements in the two orthogonal directions using a rigid body rotation to produce a zero beam end deflection, see Fig. 2(b). Thus both quantities represent resultants at 45 degrees to the main structural axis. The behavior of one specimen, BCJ5, will be described in some detail, and only differences in behavior for the other specimens will be noted.

Effect of Beam Size

Three specimens with different beam widths and without floor slabs were tested to investigate the effect of framing beam size on joint behavior. The intent was to clarify the confining effect provided by the loading beams to the joint core.

A) BCJ5 - (Beams = 13 x 18 in.) The resulting moment-interstory displacement plot for BCJ5 is shown in Fig. 5. The plot clearly shows the large losses of strength and stiffness (particularly after LS 68) with cycling that characterized all the specimens tested. The beams achieved their flexural capacity when loading to the first peaks at the first two deflection levels (LS 12 and 68), and reached the descending portion of the strength envelope by the time the third deflection level (LS 124) was reached. Cycling at the same deflection level resulted in strength losses of about 20% for the first and almost 30% for the second deflection level. The backbone stiffnesses for the first deflection level were about 20% of the measured uncracked stiffness of the subassembly, and dropped about 15-20% with cycling at the first and about 25% at the second deflection level. The severe pinching of the loops observed at all deflection levels indicates poor energy dissipation characteristics. This pinching is due primarily to the slippage of the top longitudinal bars and the yield penetration into the joint area. The very low stiffnesses near the undeformed position are a result

of the very wide cracks at the beam-column interface; until these cracks closed the stiffness was not regained. With cycling, progressively larger deformations were needed to regain stiffness and strength.

The observed behavior of BCJ5 indicated that the first joint shear cracking occurred at a shear stress level of about 700 psi, or about $10.5\sqrt{f'c}$. By the first peak, LS 12, the beams showed extensive flexural and flexural-shear cracking, and the main crack at the column face extended for about 70% of the beam depth. With the reversal of loading, to LS 24, the cracks extended through the full depth of the beams and a crossing pattern of shear cracks at the joint corners were clearly visible. Little additional cracking occurred after LS 68, although the existing cracks continued to widen with cycling

BCJ5 did not exhibit a clear shear failure, although nominal shear stresses as high as 1800 psi were applied to the joint. The behavior degraded due to the slippage of the top bars during the first deflection level and of the bottom bars during the second deflection level. The yield penetration into the joint and the extensive shear cracking also contributed significantly to the degradation of performance with cycling for BCJ5.

B) BCJ12 (Beams = 18 x 18 in.) The behavior of BCJ12, shown in Fig. 6, was very similar to that of BCJ5. The specimens differed only in the beam width and the fact that the outside longitudinal beam bars did not pass through the confined joint core. The strength and hysteretic trends are similar, with a slight increase in moment capacity for BCJ12 due to the increase in internal moment arm. The cracking patterns evidenced less column flexural cracking and beam shear-flexural cracking for BCJ12, but the cracks at the column face seemed wider. The top bars began to slip at LS 24, and considerable yielding was present at the critical section.

C) BCJ11 (Beams = 8.75 x 18 in.) The behavior of BCJ11 was very different from those of BCJ5 and BCJ12, see Figs. 7 and 8. BCJ11 showed an early failure due to the crushing and spalling of the column and joint corners in compression. This early loss of section resulted in a substantial drop in column moment capacity and did not allow the beams to reach their yield strength. The deformations began to concentrate in the joint area, and the critical corner column bars lost all bond through the joint; by LS 68, the corner column bars could be seen forming hinges at the top and bottom of the joint. The specimen showed very undesirable behavior, and showed the importance of the beam size in helping to confine the joint corners.

Effect of Floor Slabs

Most R.C. frames have monolithic floor slabs cast with the beams and columns. There are no provisions in current codes to account for the added flexural capacity provided by these members. While it is safe to ignore their contribution when considering gravity loads, their additional flexural capacity might result in a beam

overstrength with respect to the column under lateral loads.

D) BCJ8 (Beams = 13 x 18 in, no slab) The behavior of BCJ8 was very similar to that of BCJ5 despite the absence of a column axial load, see Fig. 9 . The most significant observed difference was the increase in flexural cracking in the column and a slightly higher rate of stiffness loss, both explainable by the elimination of the axial load. The beam longitudinal reinforcement began to slip earlier in the load history (LS 10), but the magnitude of slip was similar after LS 24.

E) BCJ9 (Beams = 13 x 18 in., slab =3.75 in thick) - BCJ9 showed two distinct types of behavior, see Fig. 10. For the first deflection level (LS 1 to 60), the beams acted as T-sections, with almost the full width of the slab being effective in both tension and compression. For the second and third deflection levels, the cracks at the beam-slab interfaces became very large and the slab only contributed in tension. As cycling progressed and the usual loss of column section began to occur, a plastic hinge began to form in the joint area rather than in the beams or column. This was due primarily to the increase in stiffness of the slab-beam system with respect to the column, and possibly to the larger shear forces acting on the joint. It was clear throughout the test that the additional stiffness provided by the slab also helped transfer some of the load to the transverse beams in torsion. The cracking near the joint area was more distributed, and more inclined cracking (possibly a combination of shear and torsional effects) was evident.

CONCLUSIONS

This experimental program demonstrated that:

1) the beam size can have a significant effect on joint performance. Beams covering at least 85% of all joint faces can be counted to provide significant confinement to joints loaded biaxially. For this additional confinement to be effective, the unconfined corners of the column and joint must be covered by the framing beams. The use of very narrow beams should be discouraged when substantial biaxial loads are expected.

2) a floor slab can have a major influence in the flexural capacity of the beams framing into a joint; this additional capacity results in higher shears for the joint and in less column-to-beam flexural overstrength than anticipated from the design calculations. It is essential that the designer be aware of the impact that a slab can have on overall joint behavior and that a conservative estimate for the effective slab width be used when calculating the flexural capacity of the slab-beam system.

3) the shear strength of interior beam-column joints is very high. Shear stresses on the order of 25 to $30\sqrt{f'c}$ were resisted without an apparent shear failure, and the shear strength was recovered as the deformations increased from one deflection level to

the next. The drop in strength with cycling at the same deformation level was more a result of bar slippage than joint shear cracking.

4) the bond conditions can have a significant effect on joint performance. The anchorage length for the top longitudinal beam bars (15 bar diameters) was insufficient to prevent slippage even at low deformation levels; those of the bottom bars (20 bar diameters) showed better performance at the first deflection level, but did not prevent significant slip with cycling and increased deformations.

ACKNOWLEDGEMENTS

The work described herein was carried out at the Ferguson Structural Engineering Laboratory of the University of Texas at Austin, as part of the author's dissertation program under the supervision of Dr. J.O. Jirsa. The work was supported by the National Science Foundation under Grants Numbers ENV-77-20816 and PRF-7720816.

REFERENCES

- 1) Jirsa, J.O., and Meinheit, D.F., The Shear Strength of Beam-Column Joints, Technical Report CESRL 77-1, The University of Texas at Austin, January 1977.
- 2) Paulay, T., Park, R., and Priestley, M.J.N., Reinforced Concrete Beam-Column Joints under Seismic Actions, ACI Journal, 75 (11) pp. 585-593 , November 1978
- 3) Viwathanatepa, S., Popov, E.P., and Bertero, V.V., Seismic Behavior of Reinforced Concrete Beam-Column Subassemblages, Technical Report UCB/EERC 79-14, University of California at Berkeley, June 1979
- 4) Bertero, V.V., Seismic Behavior of Structural Concrete - Linear Elements and their Connections, Symposium on Structural Concrete under Seismic Actions, C.E.B., Rome, May 1979
- 5) Leon, R.T., The Influence of Floor Members on the Behavior of Reinforced Concrete Beam-Column Joints Subjected to Severe Cyclic Loading, PhD thesis, The University of Texas at Austin, December 1983

Table 1 - Specimen Size and Reinforcement

Specimen	Beam Size	Beam Reinf. Top	Beam Reinf. Bottom	Column Reinf.	Axial Load	Moment Ratio	Type
BCJ5	13 x 18	3 # 8	3 # 6	12 # 9	300	1.28	Regular
BCJ11	8.8 x 18	2 # 10	2 # 8	9 # 11	300	1.25	Narrow
BCJ12	18 x 18	3 # 8	3 # 6	12 # 9	300	1.13	Wide
BCJ8	13 x 18	3 # 8	3 # 6	12 # 9	0	1.26	No slab
BCJ9	13 x 18	3 # 8	3 # 6	12 # 9	0	1.16	Slab

All units are inches and kips; all column 15 x 15 in.

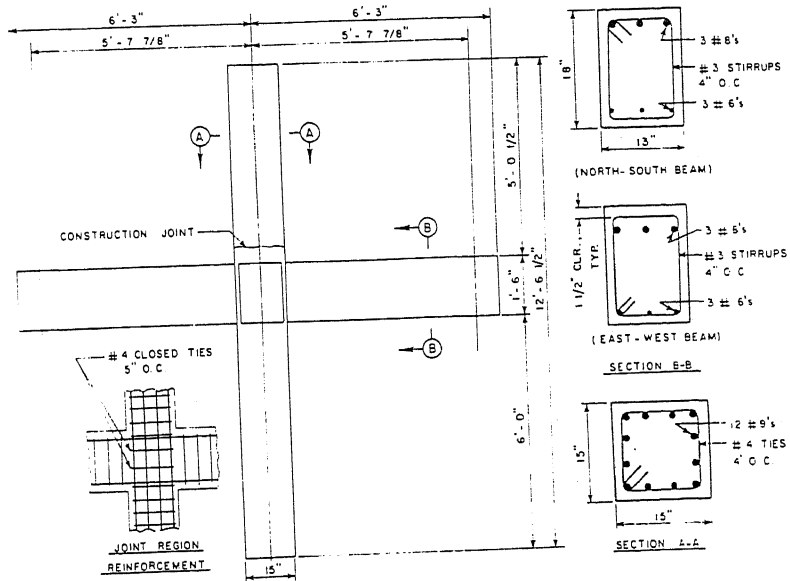
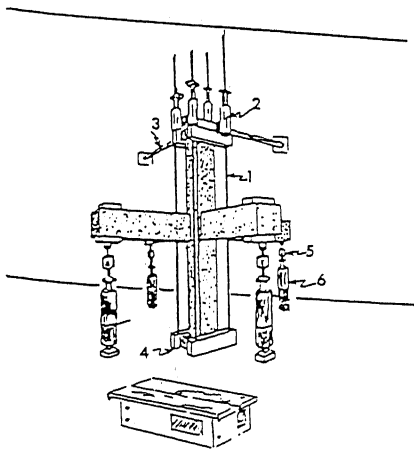


Fig. 1 - Specimen size and reinforcement



- (1) Axial load rods
- (2) Axial load rams
- (3) Shear struts to reaction wall
- (4) Semi-fixed base
- (5) Load cell
- (6) Loading rams

Fig. 2 - Test setup

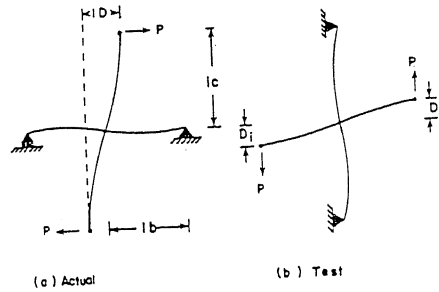


Fig. 3 - Deflected shapes

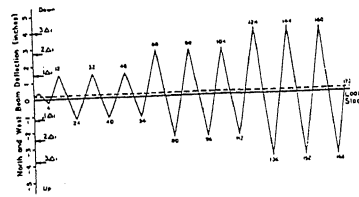


Fig. 4 - Load history

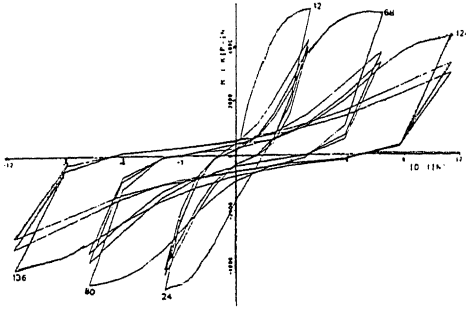


Fig. 5 - M vs. ID (BCJ5)
 M = 2000 K-in/division
 ID = 3 in/division

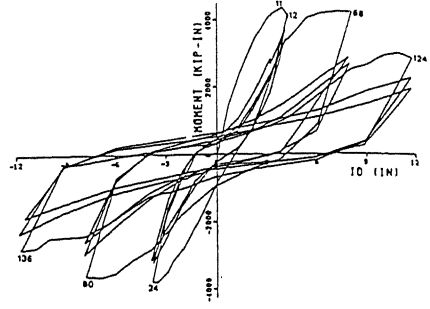


Fig. 6 - M vs. ID (BCJ12)

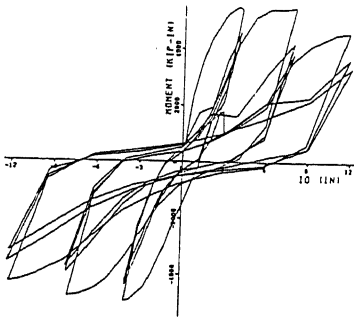


Fig. 7 - M vs. ID (BCJ11)

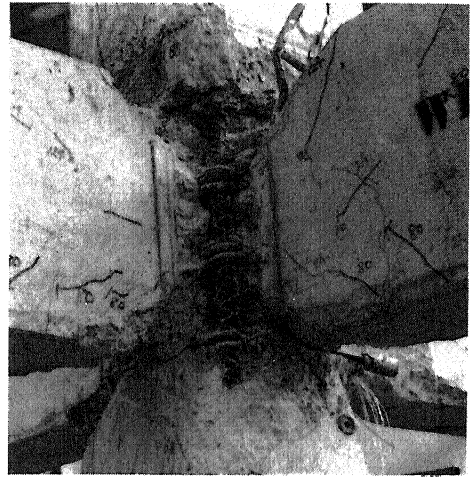


Fig. 8 - BCJ11 at LS124

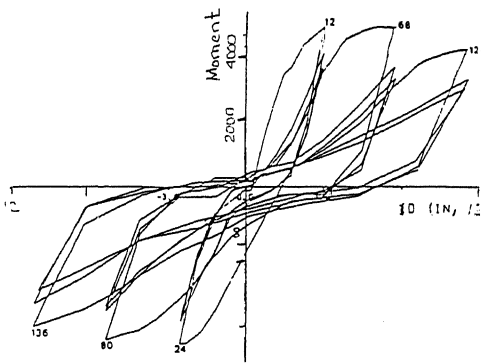


Fig. 9 - M vs. ID (BCJ8)

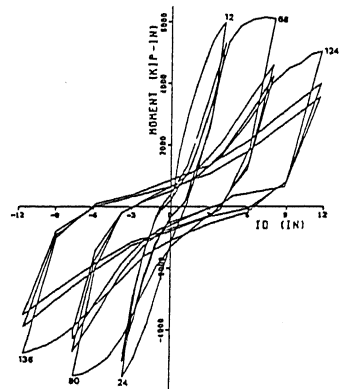


Fig. 10 - M vs. ID (BCJ9)